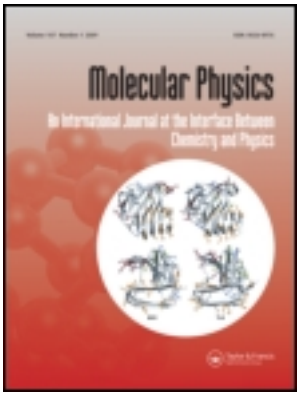

Molecular Physics
Publication details, including instructions for authors and subscription information:
http://www.tandfonline.com/loi/tmph20

Structure, thermodynamics, and orientational correlations of the nematogenic hard ellipse fluid from the Percus-Yevick equation

D.A. Ward [a] & F. Lado [b]

[a] Physics Department, Florida Southern College, Lakeland, Florida, 33802, U.S.A.

[b] Physics Department, North Carolina State University, Raleigh, North Carolina, 27695-8202, U.S.A.

Available online: 26 Oct 2007

To cite this article: D.A. Ward & F. Lado (1988): Structure, thermodynamics, and orientational correlations of the nematogenic hard ellipse fluid from the Percus-Yevick equation, Molecular Physics, 63:4, 623-638

To link to this article: http://dx.doi.org/10.1080/00268978800100431

MOLECULAR PHYSICS, 1988, VOL. 63, NO. 4, 623–638

Structure, thermodynamics, and orientational correlations of the nematogenic hard ellipse fluid from the Percus–Yevick equation

by D. A. WARD
Physics Department, Florida Southern College,
Lakeland, Florida 33802, U.S.A.

and F. LADO
Physics Department, North Carolina State University,
Raleigh, North Carolina 27695-8202, U.S.A.

(*Received 18 June 1987; accepted 13 November 1987*)

The Percus–Yevick equation is solved for a fluid of hard ellipses in two dimensions. The correlation functions, including the orientation correlation function, are expanded in a set of orthogonal functions and the expansion coefficients are obtained by an iterative algorithm. Pressure and compressibility values are also determined. Orientational ordering is observed, but the isotropic-nematic phase transition observed by Vieillard-Baron (1972, *J. chem. Phys.*, **56,** 4729) is not.

1. Introduction

Molecular liquids interacting through angle-dependent pair potentials may exhibit liquid crystalline behaviour. Liquid crystals are orientationally ordered fluids, the simplest of which is the nematic liquid crystal [1]. In the nematic phase, the molecular axes, on average, line up preferentially along a common direction. The density at which this takes place is called the isotropic-nematic (I-N) phase transition density.

The I–N phase transition in 3 dimensions is said to be 'weakly' first order, in that the density, entropy, and volume changes at the transition are quite small when compared to the corresponding changes at the freezing transition [2]. The existence of the I–N phase transition was predicted separately by Maier and Saupe [3] and Onsager [4]. Though each of these studies centred on different physical factors, they each managed to predict the I–N phase transition from a statistical-molecular viewpoint.

The focus of the present work is to investigate the thermodynamic variables and I–N phase transition of a two-dimensional nematogenic fluid. Such a fluid may be envisioned as a plane of elongated molecules. This monolayer might be formed by absorbing elongated molecules onto a smooth substrate.

Whether or not a true nematic phase can exist in 2 dimensions has been a matter of debate [5–7] which has not been resolved by the various Monte Carlo (MC) simulations currently available [6–8]. Indeed, there are reasons to believe that true

phase transitions cannot even exist in 2 dimensions [9]. Our purpose here is not to answer these important questions, but to apply the integral equation theory of classical liquids [10] to the two-dimensional hard ellipse fluid.

We should note, however, that the intermolecular pair potential seems to play a key role in determining whether or not one may expect to find long-range orientational order in a two-dimensional fluid of elongated molecules. It has been demonstrated by Straley [5] that no true long-range order can exist in two-dimensional nematics if the intermolecular pair potential is separable.

A separable pair potential is one which is factorizable into distance-dependent and angle-dependent parts. Thus, in seeking the existence of long-range orientational order one must look to systems interacting through nonseparable pair potentials, for which long-range order has not been excluded. The simulations of Tobochnik and Chester [6] of both separable and nonseparable potentials seem to confirm the conclusions of Straley, for those potentials which they chose. Their results suggested that true long-range order exists in the system possessing a nonseparable interaction, while the nonseparable system fails to exhibit this order.

In a recent publication, Frenkel and Eppenga [8] report a MC study which focuses on the ordering of a two-dimensional fluid of hard needles. Though this is a nonseparable system, their simulations suggest that the two-dimensional hard needle fluid possesses only a 'quasi-long-range order' due to the fact that the nematic order parameter vanishes in the thermodynamic limit. Further, the order-parameter correlation functions they studied seem to decay algebraically.

MC data have been obtained for the hard ellipse fluid in two dimensions by Vieillard-Baron [19]. The simulation was of a system of ellipses with a ratio of long-to-short axes $a/b = 6$. This simulation seems to indicate that the I–N phase transition is of first order, as the equation of state (EOS) exhibits a small discontinuity between the isotropic and nematic phases. This is in direct contrast to the MC data of Frenkel and Eppenga [8] which showed that it was unlikely that the I–N phase transition of the hard ellipse system was of first order.

It is desirable at this point to bring the formalism of integral equation theory to this problem. Integral equation theory has been applied to the study of a variety of systems interacting via angle-dependent potentials [11–13], but relatively few studies have centred on nematic systems. In a recent study [14], the RHNC integral equation was applied to several nematic liquid crystal models in three dimensions, yielding very encouraging results.

The only two-dimensional applications of integral equations to nematics seem to be those of Chakravarty and Woo [15]. The intermolecular pair potentials they studied were angle-dependent with a soft core. Their results indicated that both nematic and isotropic phases become possible beyond a particular number density. It should be mentioned here that in their study Chakravarty and Woo were forced to assume that the isotropic pair correlation function remained isotropic through the phase transition. This was done in order to make the numerical work more tractable.

It is thus desirable to straightforwardly apply the integral equation theory to a nematogen with few restricting assumptions. The most general method currently available for this task was developed and used by Lado [16–18]. Lado's technique will be applied here to the two-dimensional fluid of hard ellipses, which possesses a nonseparable potential. The results reported here were obtained by solving the Percus–Yevick (PY) integral equation for the three elongations: $a/b = 2$, 4, and 6.

This was done at a variety of number densities, and the EOS, compressibility, and orientational coefficients were found for each case. In contrast to the MC study of Vieillard-Baron [19], we find that the PY equation fails to predict a first order I–N phase transition.

2. General formulation

2.1. *Linear molecules in two dimensions*

The key task in applying integral equation theory is in iteratively solving the Ornstein–Zernike (OZ) equation [10]

$$h(12) = g(12) - 1 = c(12) + \frac{\rho}{\Omega}\int d3c(13)h(32), \tag{1}$$

coupled with the closure relation

$$c(12) = h(12) - \ln\{g(12)\exp[\beta\Phi(12)]\} + B(12), \tag{2}$$

where $c(12)$, $h(12)$, and $g(12)$ are the direct, total, and pair correlation functions, respectively, ρ is the particle number density, and $\beta = 1/kT$. In 2 dimensions the integration over the position and angular coordinates of particle 3 is $d3 = d\mathbf{r}_3\, d\theta_3$, with

$$\Omega = \int d\theta_3 = 2\pi. \tag{3}$$

The unknown function $B(12)$ may be shown to equal a class of diagrams known as bridge diagrams and is thus called the bridge function. In order to iteratively solve equations (1) and (2), it is necessary to adopt an approximation for $B(12)$. As was mentioned earlier, in this work the PY approximation [10] was chosen. The PY direct and pair correlation functions are

$$c(12) = \{1 + S(12)\}\{\exp[-\beta\Phi(12)] - 1\}, \tag{4}$$

and

$$g(12) = \{1 + S(12)\}\exp[-\beta\Phi(12)], \tag{5}$$

where $S(12) = h(12) - c(12)$ is the series function. In practice, it is preferred to work with the series function as it is more slowly-varying and thus is more suitable for numerical manipulation than $h(12)$.

We shall retain $B(12)$ in our development below for the sake of generality. In terms of $S(12)$, the OZ equation and closure relation become

$$S(12) = \frac{\rho}{2\pi}\int c(13)[S(32) + c(32)]\, d3, \tag{6}$$

$$c(12) = g(12) - S(12) - 1, \tag{7}$$

with the pair correlation function becoming

$$g(12) = \exp[-\beta\Phi(12) + S(12) + B(12)]. \tag{8}$$

In the absence of any external potentials, the origin and orientation of the coordinate frame is essentially arbitrary. As a consequence, the correlation functions will depend only upon the intermolecular separation, r, and molecular orientations. Thus, for example, $S(12) = S(r, \theta_1, \theta_2)$, with all other correlation functions being

similar in form. We choose a coordinate system in which particle 1 is placed at the origin, with particle 2 at a distance r from the origin on the y axis. The orientation angles θ_1 and θ_2 are measured with respect to the intermolecular axis.

The iterative solution of equations (6)–(8) involves functions of three variables and is thus cumbersome to deal with numerically. The now-standard means of overcoming this difficulty is to expand the correlation functions in a complete set of orthogonal functions [16, 21]. After Caillol *et al.* [22], we expand $S(12)$ as

$$S(12) = \sum_{m,j=-\infty}^{\infty}\sum S(r; m, j) \exp [i(m\theta_1 + j\theta_2)], \tag{9}$$

which reduces the problem to one in which one must numerically solve for the one-variable functions $S(r; m, j)$.

The correlation functions are invariant with respect to a reflection of linear particles about the intermolecular axis. Hence,

$$S(r, \theta_1, \theta_2) = S(r, 2\pi - \theta_1, 2\pi - \theta_2). \tag{10}$$

This symmetry applied to (9) yields

$$S(12) = \sum_{m,j} S(r; m, j) \cos (m\theta_1 + j\theta_2), \tag{11}$$

where

$$S(r; m, j) = \frac{1}{4\pi^2} \int_0^{2\pi} d\theta_1 \int_0^{2\pi} d\theta_2 \, S(r, \theta_1, \theta_2) \cos (m\theta_1 + j\theta_2), \tag{12}$$

with $S(r; m, j) = S(r; -m, -j)$.

Thus, given an initial input set of the S-coefficients, $S(r; m, j)$, $S(12)$ may be found via (11). Then, $S(12)$ may be used in (8) in order to obtain $g(12)$. An application of (12) to $g(12)$ will yield the g-coefficients. The c-coefficients may next be found. Inserting the series representation of each correlation function into (7) yields

$$c(r; m, j) = g(r; m, j) - S(r; m, j) - \delta_{m,0}\,\delta_{j,0}. \tag{13}$$

Once the $c(r; m, j)$ are obtained, the final task is to obtain a new set of the $S(r; m, j)$ via the OZ equation (6), thus completing one iteration. This involves reducing the OZ equation by Fourier transformation as in [16]. The Fourier transform of $S(12)$ is given formally by

$$\tilde{S}(12) = \int S(12) \exp [i\mathbf{k} \cdot \mathbf{r}] \, d\mathbf{r}. \tag{14}$$

Inserting (6) into (14) yields

$$\tilde{S}(12) = \frac{\rho}{2\pi} \int d\theta_3 \tilde{c}(13)[\tilde{S}(32) + \tilde{c}(32)]. \tag{15}$$

We choose to write the transformed functions in (15) in a new coordinate frame in which the angles denoting the molecular orientations are measured with respect to $\mathbf{k}$. Thus

$$\tilde{S}(12) = \tilde{S}(k, \theta_1', \theta_2') = \sum_{m,j} \tilde{S}(k; m, j) \cos (m\theta_1' + j\theta_2'), \tag{16}$$

where the prime denotes that the angles are measured with respect to $\mathbf{k}$.

Placing the appropriate series for each Fourier transform into (15) and effecting the angular integration yields

$$\tilde{S}(k;\, p,\, j) = \rho \sum_{m=-\infty}^{\infty} \tilde{c}(k;\, p,\, -m)[\tilde{S}(k;\, m,\, j) + \tilde{c}(k;\, m,\, j)]. \tag{17}$$

Defining a 'c-minus' matrix by $\tilde{c}^{-}(k;\, p,\, m) = \tilde{c}(k;\, p,\, -m)$ enables one to write the OZ equation (17) in the matrix form

$$\tilde{\mathbf{S}} = \rho\tilde{\mathbf{c}}^{-}[\tilde{\mathbf{S}} + \tilde{\mathbf{c}}], \tag{18}$$

which may be solved for $\tilde{\mathbf{S}}$ to yield

$$\tilde{\mathbf{S}} = \rho\{\mathbf{I} - \rho\tilde{\mathbf{c}}^{-}]^{-1}\tilde{\mathbf{c}}^{-}\tilde{\mathbf{c}}, \tag{19}$$

where $\mathbf{I}$ denotes the identity matrix. A Fourier inversion of the terms in $\tilde{\mathbf{S}}$ will result in a new set of S-coefficients, thus ending the iteration. The new set would be used as the input for a new iteration, if convergence was not obtained.

The final task is to link the expansion coefficients $\tilde{S}(k;\, m,\, j)$ to the $S(r;\, m,\, j)$, recalling that these coefficients represent expansions in two different coordinate frames. The key difference between these two frames is a simple rotation through the angle between $\mathbf{r}$ and $\mathbf{k}$, which we shall call α. Thus, $\theta_j = \theta'_j + \alpha$, where $j = 1$ or 2. Making this substitution into the expansion (11) for $S(12)$ and effecting the Fourier transform (14), one can show that

$$\tilde{S}(k;\, m,\, j) = 2\pi i^{(m+j)} \int_0^{\infty} S(r;\, m,\, j) J_{m+j}(kr) r\, dr, \tag{20}$$

where J_p denotes the pth order Bessel function of the first kind [23],

$$J_p(x) = \frac{i^{-p}}{\pi} \int_0^{\pi} \cos(p\phi) \exp[ix \cos\phi]\, d\phi. \tag{21}$$

One may invert (20) to obtain the $S(r;\, m,\, j)$ by using [23]

$$\delta(r - r') = r \int_0^{\infty} J_p(kr) J_p(kr') k\, dk, \tag{22}$$

which yields

$$S(r;\, m,\, j) = \frac{1}{2\pi i^{(m+j)}} \int_0^{\infty} \tilde{S}(k;\, m,\, j) J_{m+j}(kr) k\, dk. \tag{23}$$

(It is of interest to note that the $\tilde{S}(0;\, m,\, j)$ and $S(0;\, m,\, j)$ vanish for $m + j \neq 0$, owing to the fact that $J_p(0) = 0$ for $p \neq 0$ [23].)

Equations (20) and (23) complete the algorithm. In the next section, we shall specialize to a fluid composed of non-polar molecules and summarize the algorithm.

2.2. *The non-polar case*

The fluid studied in this work consisted of N identical, linear, non-polar molecules. By the term non-polar, we mean that one cannot distinguish between a molecule's 'head' and its 'tail'. This extra symmetry may be used to simplify the

series representations of the correlation functions. The non-polar linear molecule has the added symmetry

$$S(r, \theta_1, \theta_2) = S(r, \theta_1 + \pi, \theta_2) = S(r, \theta_1, \theta_2 + \pi). \tag{24}$$

Using the series form of $S(12)$ along with the symmetry represented in (24), one may easily show that the double-sum in (11) and (16) has non-zero coefficients for even m and j only. Thus, we may write

$$S(r, \theta_1, \theta_2) = \sum_{m,j=-\infty}^{\infty} S(r; m, j) \cos(2m\theta_1 + 2j\theta_2). \tag{25}$$

Similar series exist for the other correlation functions.

The relations developed in § 2.1 contain all the necessary elements for iteratively solving for the coefficients $S(r; m, j)$. Below, for the sake of clarity, we summarize an entire iteration for a new set of $S(r; m, j)$s for the fluid of linear, non-polar molecules in 2 dimensions. All the appropriate modifications due to symmetry have been made.

(1) Input an initial set of $S(r; m, j)$s.

(2) Compute the series function using

$$S(r, \theta_1, \theta_2) = \sum_{m,j} S(r; m, j) \cos(2m\theta_1 + 2j\theta_2). \tag{26}$$

(3) Compute the pair correlation function,

$$g(r, \theta_1, \theta_2) = \exp[-\beta\Phi(r, \theta_1, \theta_2) + S(r, \theta_1, \theta_2) + B(r, \theta_1, \theta_2)]. \tag{27}$$

(4) Compute the g-coefficients,

$$g(r; m, j) = \frac{1}{\pi^2} \int_0^{\pi} d\theta_1 \int_0^{\pi} d\theta_2\, g(r, \theta_1, \theta_2) \cos(2m\theta_1 + 2j\theta_2). \tag{28}$$

(5) Compute the c-coefficients,

$$c(r; m, j) = g(r; m, j) - S(r; m, j) - \delta_{m,0}\,\delta_{j0}. \tag{29}$$

(6) Compute the transformed c-coefficients,

$$\tilde{c}(k; m, j) = 2\pi(-1)^n \int_0^{\infty} c(r; m, j) J_{2n}(kr) r\, dr, \tag{30}$$

where $n = m + j$.

(7) Determine the new $\tilde{S}(k; m, j)$s via the matrix OZ equation,

$$\tilde{\mathbf{S}} = \rho[\mathbf{I} - \rho\tilde{\mathbf{c}}^{-}]^{-1}\tilde{\mathbf{c}}^{-}\tilde{\mathbf{c}}. \tag{31}$$

(8) Invert the $\tilde{S}(k; m, j)$s to obtain the new $S(r; m, j)$s,

$$S(r; m, j) = \frac{1}{2\pi(-1)^n} \int_0^{\infty} \tilde{S}(k; m, j) J_{2n}(kr) k\, dk, \tag{32}$$

where $n = m + j$.

This completes one full iteration for the S-coefficients. The new set of coefficients is used as the input for the next iteration until convergence is obtained.

3. Thermodynamic relations

The fluid studied in this work is composed of infinitely-hard, linear molecules. The thermodynamic quantities of interest will be the pressure, p, and isothermal compressibility, χ. The only contribution to the total internal energy, E, is purely kinetic, as the interaction energy is zero for all allowed molecular configurations.

The pressure and isothermal compressibility are given quite generally by [10]

$$\frac{\beta p}{\rho} = 1 - \frac{\rho}{2V\kappa\Omega^2} \int r_{12}\beta \frac{\partial \Phi(12)}{\partial r_{12}} g(12)\, d1\, d2, \tag{33}$$

and

$$\frac{\rho\chi}{\beta} = 1 + \frac{\rho}{V\Omega^2} \int [g(12) - 1]\, d1\, d2, \tag{34}$$

where $\kappa = 2$ or 3, for two or three dimensions, respectively. The constant Ω is given by (3), and V denotes the area.

An alternative expression for the compressibility which is more stable for numerical calculation is [24]

$$\frac{\rho\chi}{\beta} = [1 - \rho\tilde{c}(0; 0, 0)]^{-1}, \tag{35}$$

where $\tilde{c}(0; 0, 0)$ denotes the transform of $c(r; 0, 0)$ evaluated at the origin, $k = 0$.

The pressure (33) may be simplified somewhat, owing to the fact that the particles considered here are infinitely-hard and possess no other interactions. Let $r_0(\theta_1, \theta_2)$ denote the distance of closest approach of two particles with orientations θ_1 and θ_2. At a given orientation, two hard particles may never be closer than this 'hard-core' distance. The pressure may be written in terms of the hard-core distance as [25]

$$\frac{\beta p}{\rho} = 1 + \frac{\rho}{2\pi} \int_0^\infty d\theta_1 \int_0^\pi d\theta_2\, r_0^2(\theta_1, \theta_2) g[r_0(\theta_1, \theta_2), \theta_1, \theta_2], \tag{36}$$

for our fluid of linear, infinitely-hard, and non-polar molecules in 2 dimensions. Thus, the excess pressure due to molecular exclusion is a functional of the hard-core value of the pair correlation function. The pressure values reported in subsequent sections are computed using (36).

4. The orientation correlation function

A nematic liquid's orientational order is often characterized by the value of a nematic order parameter and a singlet distribution function, $f(\theta)$ [1]. The angle θ is

specified with respect to some externally imposed 'director' and $f(\theta)$ is calculated in a mean field approximation.

But, in the absence of any external fields the properties of the molecular fluid depend solely on the relative orientations and relative separations of the constituent molecules. Thus, ordering should properly be sought in terms of pair correlations. The function describing the total angular correlation between a pair of molecules will be termed the orientation correlation function (OCF).

The OCF was first obtained and applied by Lado [18] to a fluid of hard dumbbells in 3 dimensions. In 2 dimensions, the OCF is defined by

$$G(\theta, \theta') = \frac{1}{N}\left\langle \left[\sum_{j=1}^{N} \delta(\theta' - \theta_j) - \frac{N}{2\pi}\right]\left[\sum_{i=1}^{N} \delta(\theta - \theta_i) - \frac{N}{2\pi}\right]\right\rangle, \tag{37}$$

where the angular brackets denote an average in the canonical ensemble and the singlet distribution for molecular orientations,

$$f(\theta) = \left\langle \sum_{j=1}^{N} \delta(\theta - \theta_j)\right\rangle = \frac{N}{2\pi}, \tag{38}$$

is uniform.

If Lado's procedure [18] is explicitly followed for simplifying the OCF in (37), one obtains [26]

$$G(\theta_{12}) = \sum_{j=1}^{\infty} G_j \cos(2j\theta_{12}), \tag{39}$$

where $\theta_{12} = \theta_1 - \theta_2$. The orientational coefficient, G_j, are given by

$$G_j = \frac{\rho}{\pi}\tilde{h}(0; j, -j), \tag{40}$$

where the $\tilde{h}(0; j, -j)$ are the transformed coefficients of $h(12)$ evaluated at the origin, $k = 0$. By virtue of the definition (1) of $h(12)$, $\tilde{h}(0; j, -j) = \tilde{g}(0; j, -j)$ for the terms appearing in (39), namely $j \geqslant 1$. These coefficients are readily obtainable from the integral equation solution outlined in § 2. Note that for low density or systems of spherical molecules the G_j vanish, revealing no orientational order. Thus, the G_js play the role of order parameters.

It should be mentioned here that (39) is indeed applicable to the polar case if one replaces the $2j$ in the cosine term with j, as in writing (39) the added symmetry discussed in § 2.2 was used.

5. The hard ellipse potential and reduced variables

The hard ellipse molecule is specified by the lengths of its semimajor axis, a, and semiminor axis, b. The intermolecular separation is denoted by r, and the angle describing a molecule's orientation is measured between the semimajor axis and r. For a given orientation, the value of r at contact between two molecules, $r_0(\theta_1, \theta_2)$, is used to describe the molecular pair potential. The pair potential is given by

$$\begin{aligned} \Phi(12) &= \infty, \quad r < r_0(\theta_1, \theta_2) \\ &= 0, \quad \text{otherwise.} \end{aligned} \tag{41}$$

for $r < 2b$ there is overlap for all orientations, while for $r > 2a$ the potential is zero at all orientations.

The contact distance, $r_0(\theta_1, \theta_2)$, for hard ellipses is obtained from the roots of the 'contact function' derived by Vieillard-Baron [19]. The contact function, $\Psi(r, \theta_1, \theta_2)$, is given by

$$\Psi(r, \theta_1, \theta_2) = 4(f_1^2 - 3f_2)(f_2^2 - 3f_1) - (9 - f_1 f_2)^2, \tag{42}$$

wherein

$$f_j = 1 + Z - \left[\frac{r}{a}\cos\theta_j\right]^2 - \left[\frac{r}{b}\sin\theta_j\right]^2, \tag{43}$$

$$Z = 2 + \left[\frac{a}{b} - \frac{b}{a}\right]\sin^2(\theta_2 - \theta_1), \tag{44}$$

with $j = 1, 2$.

The contact function is zero for a given orientation whenever the two ellipses are tangent exteriorly or interiorly. Consequently, the contact distance is obtained by selecting the largest root of the contact function for a given orientation. The largest root of (42) was obtained via the Newton's rule iteration [27]. The criterion for convergence between the input and output values of the estimated root was

$$|r_{0_{in}} - r_{0_{out}}| < 0{\cdot}001. \tag{45}$$

As there is no contact for r larger than $2a$, the iteration was begun at $r = 2a$ and terminated when the first root was found, as this largest root corresponds to the contact distance. Armed with a set of values for the contact distance at a variety of orientations, (41) is then used to determine the potential, which is needed in (27). These values are also critical in determining the pressure (36).

The reduced variables used in this work to characterize the fluid of hard ellipses are:

$$R = r/2a, \tag{46}$$

$$\rho^* = 4\rho ab, \tag{47}$$

$$l = a/b, \tag{48}$$

where R, ρ^*, and l denote the reduced distance, reduced density, and elongation, respectively. The above choices were made because they go over to the reduced variables commonly used in the hard disk fluid [28], when the elongation becomes unity. The hard disk case, $l = 1$, was used as a test of the program written in this work, and it was found that the pressures computed were in agreement with those of Lado [28] to within 1 per cent.

6. Numerical results

The OZ equation was solved under a PY closure for a fluid of hard ellipses in 2 dimensions. The elongations $l = 2{\cdot}0$, $4{\cdot}0$, and $6{\cdot}0$ were studied at the densities

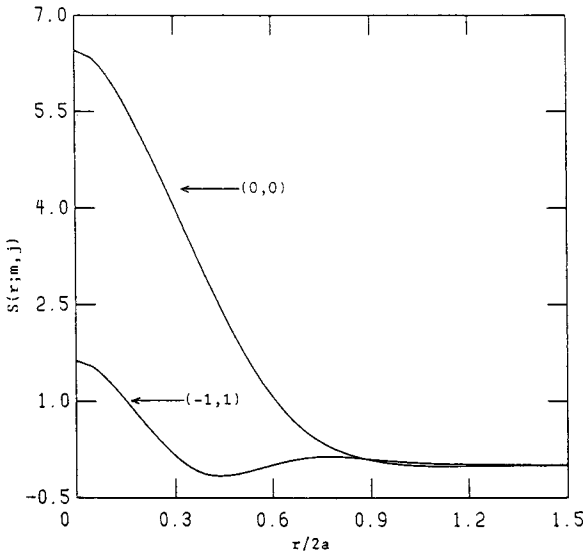

Figure 1. $S(12)$ coefficients for hard ellipses of elongation $l = 6{\cdot}0$ at the density $\rho^* = 0{\cdot}5$.

$\rho^* = 0{\cdot}1$–$0{\cdot}8$, $0{\cdot}1$–$0{\cdot}7$, and $0{\cdot}1$–$0{\cdot}66$, respectively. The densities were increased in steps of $0{\cdot}1$, except for the density region $0{\cdot}6$–$0{\cdot}66$ with an elongation of $6{\cdot}0$. This region was studied over a denser set of points in order to examine the region where Vieillard-Baron found an I–N phase transition [19].

For each elongation and density, values of the compressibility and pressure, (35) and (36), were obtained. Also found were the orientational coefficients, G_j, defined in (40), as well as the S, c, and g-coefficients. The grid sizes used are discussed in the Appendix.

A sample of the functions that appear in the calculation appears in figures 1–4 for the state $\rho^* = 0{\cdot}5$, $l = 6{\cdot}0$. The principal S-coefficients appear in figures 1 and 2.

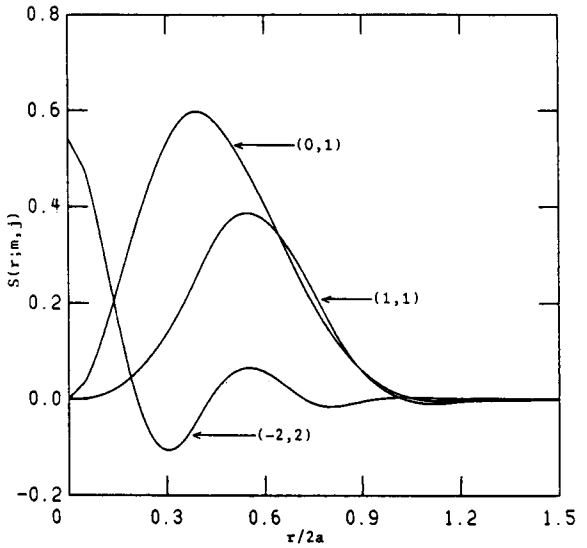

Figure 2. $S(12)$ coefficients for hard ellipses of elongation $l = 6{\cdot}0$ at the density $\rho^* = 0{\cdot}5$.

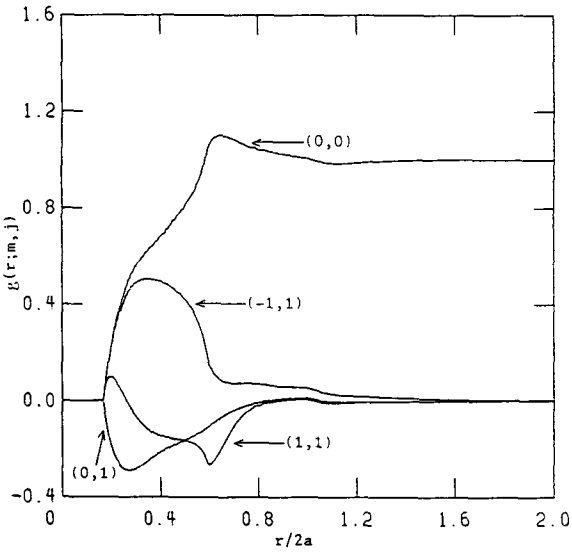

Figure 3. $g(12)$ coefficients for hard ellipses of elongation $l = 6{\cdot}0$ at the density $\rho^* = 0{\cdot}5$.

All of these coefficients exhibit their structure in the anisotropic region of the potential, $r < 2a$. Indeed, for all practical purposes, the S-coefficients vanish outside the anisotropic region. These figures, via a comparison of their scales, indicate the convergence of the $S(12)$ expansion, showing that it is not especially rapid. Figure 3 presents the principal contributors to the $g(12)$ expansion. All the g-coefficients vanish in the region $r/2a < 1/l$, as there is overlap for all orientations in this region. At $r/2a = 1{\cdot}0$, where the potential vanishes for all orientations, note the slight discontinuity in slope and the tendency for the g-coefficients to quickly take on

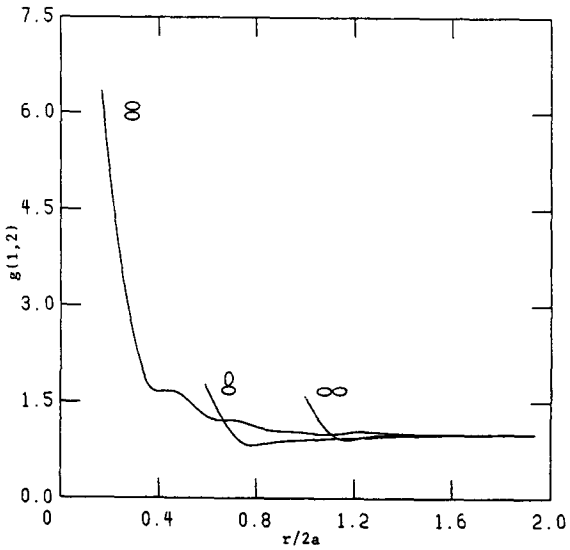

Figure 4. Cross-sections through $g(12)$ for two parallel and one T-shaped configuration for hard ellipses of elongation $l = 6{\cdot}0$ at the density $\rho^* = 0{\cdot}5$.

Table 1. The order parameters, G_j, of the hard ellipse fluid.

l	ρ^*	G_1	G_2	G_3	G_4
2·0	0·10	0·0051			
	0·20	0·0114			
	0·30	0·0190			
	0·40	0·0277	0·0021		
	0·50	0·0379	0·0032		
	0·60	0·0498	0·0048		
	0·70	0·0630	0·0069	0·0015	
	0·80	0·0781	0·0098	0·0024	
4·0	0·10	0·0219	0·0026		
	0·20	0·0492	0·0069		
	0·30	0·0817	0·0139		
	0·40	0·118	0·0234		
	0·50	0·157	0·0365	0·0097	
	0·60	0·201	0·0526	0·0155	
	0·70	0·246	0·0711	0·0231	0·0077
6·0	0·10	0·0399	0·0069		
	0·20	0·0899	0·0189	0·0054	
	0·30	0·148	0·0379	0·0118	
	0·40	0·210	0·0632	0·0215	0·0086
	0·50	0·279	0·0943	0·0351	0·0147
	0·60	0·357	0·131	0·0527	0·0234
	0·62	0·377	0·138	0·0566	0·0255
	0·64	0·395	0·147	0·0608	0·0278
	0·65	0·404	0·151	0·0629	0·0290
	0·66	0·414	0·155	0·0647	0·0301

constant values. Beyond this point, $g(r; 0, 0)$ becomes essentially unity, while the remaining g-coefficients vanish.

In figure 4 we present cross-sections of the pair correlation function for the state $\rho^* = 0{\cdot}5$, $l = 6{\cdot}0$. Two are parallel configurations and one is T-shaped, as noted on the figure. The most notable feature of these cross-sections is the lack of any well-defined peaks beyond the principal peak. Note also the large disparity in the size of the principal peaks between the orientation $\theta_1 = \theta_2 = \pi/2$ and the other two orientations.

Table 1 presents the orientational coefficients, G_j, for all the cases studied, while figures 5 and 6 present the OCF. In figure 5, the reduced density was held at 0·6 and the OCF was plotted for several elongations, while in figure 6, the reduced density was varied for a fixed elongation of 6·0. The first order I–N phase transition found by Vieillard-Baron [19] for this system occurs at a reduced density of approximately 0·65. We note from both table 1 and figure 6 that the OCF and G_j appear to vary in a continuous fashion and evidence no first order phase transition.

It should be mentioned here that no attempt was made to compare Vieillard-Baron's order parameter M [19] to our G_1, though they are directly proportional and both are used to estimate the onset of nematic order. This was due to the fact that Vieillard-Baron's M exhibited a very large degree of scatter, as he was unable to acurately determine M because of large statistical fluctuations [19].

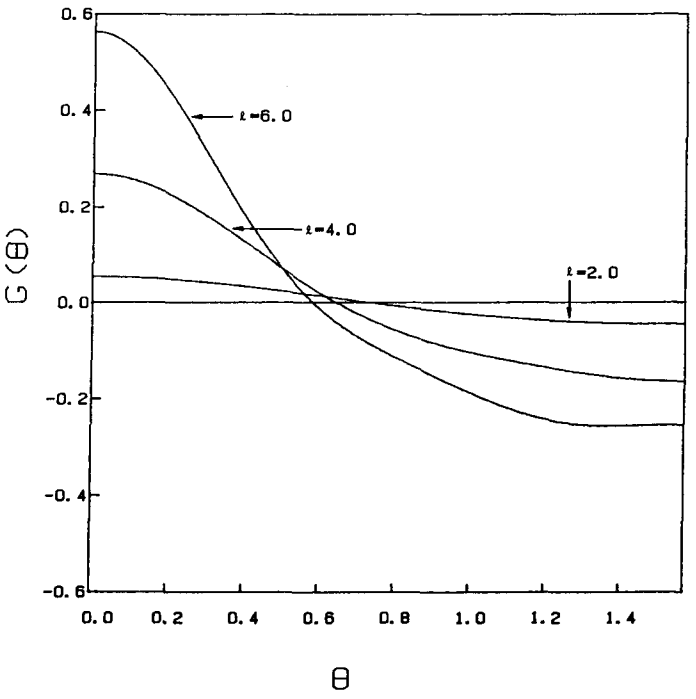

Figure 5. The orientation correlation function for the hard ellipse fluid for three elongations with density $\rho^* = 0{\cdot}6$.

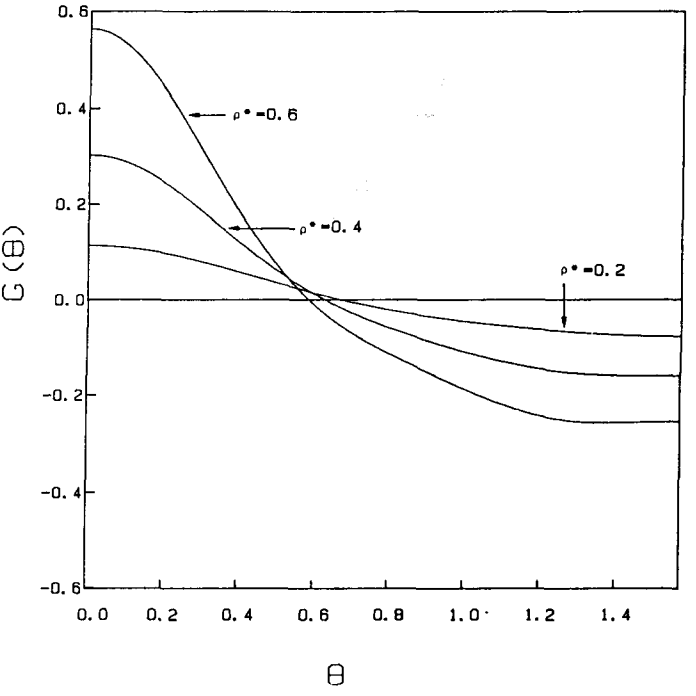

Figure 6. The orientation correlation function for the hard ellipse fluid for three densities with elongation $l = 6{\cdot}0$.

Table 2. The pressure and compressibility of the hard ellipse fluid. The compressibility was obtained from the Percus–Yevick (PY) theory, and the pressure was obtained from both the PY and scaled particle theory (SPT).

		$\beta P/\rho$		
l	ρ^*	PY	SPT	$\rho\chi/\beta$
2·0	0·10	1·20	1·20	0·704
	0·20	1·45	1·45	0·486
	0·30	1·80	1·79	0·329
	0·40	2·26	2·25	0·216
	0·50	2·91	2·91	0·138
	0·60	3·83	3·90	0·0835
	0·70	5·23	5·45	0·0478
	0·80	7·46	8·10	0·0251
4·0	0·10	1·26	1·26	0·637
	0·20	1·61	1·60	0·405
	0·30	2·09	2·06	0·255
	0·40	2·73	2·70	0·159
	0·50	3·60	3·63	0·0977
	0·60	4·84	5·03	0·0578
	0·70	6·65	7·27	0·0326
6·0	0·10	1·34	1·33	0·573
	0·20	1·80	1·77	0·336
	0·30	2·42	2·36	0·201
	0·40	3·24	3·21	0·122
	0·50	4·34	4·44	0·0730
	0·60	5·85	6·31	0·0430
	0·62	6·23	6·79	0·0384
	0·64	6·65	7·33	0·0341
	0·65	6·86	7·62	0·0322
	0·66	7·08	7·93	0·0305

Table 2 lists the thermodynamics for the cases studied, while figure 7 compares the pressure found in this work, denoted by PY, to that obtained by SPT [20] and Vieillard-Baron's MC results [19]. While the MC results clearly indicate a first order I–N phase transition, the PY theory fails to reveal such a transition. It should be noted that 25 distinct coefficients of each expansion were used in producing the thermodynamics given here. Thus, it seems quite unlikely that the addition of more coefficients would reveal this phase transition, though it would likely reduce the magnitude of the discrepancy between the MC and PY pressures at low and moderate density.

The PY results, then, tend to agree with the conclusion reached by Frenkel and Eppenga [8] that the I–N transition in the hard ellipse fluid is not of first order. Though the bulk of their paper concerned the hard needle fluid, they did carry out several runs to investigate system size dependence of nematic ordering in the hard ellipse fluid. They concluded that the hard ellipse system was not qualitatively different from the hard needle system, and that the I–N transition of a fluid of hard ellipses was not first order.

This work was supported by the National Science Foundation under Grant CHE-84-02144.

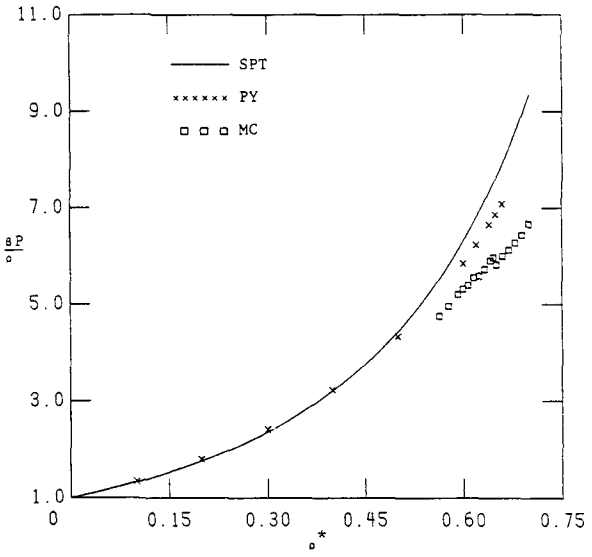

Figure 7. The equation of state of the hard ellipse fluid with elongation $l = 6{\cdot}0$.

Appendix

In (30) and (32) the computation of a Hankel transform of the form

$$\tilde{f}(k) = \int_0^\infty f(r) J_p(kr) r \, dr, \tag{A 1}$$

is required. These transforms were computed based on the Fast Hankel Transform (FHT) procedure put forth by Talman [29]. The substitutions

$$r = \exp(-y), \quad -\infty < y < \infty, \tag{A 2}$$

$$k = \exp(x), \quad -\infty < x < \infty, \tag{A 3}$$

were made, with the x and y grids chosen to be

$$x_j = x_0 + j\Delta x, \tag{A 4}$$

$$y_j = y_0 + j\Delta y, \tag{A 5}$$

where $j = 1, 2, \ldots \eta$. The specific numerical parameters used were $\Delta x = \Delta y = 0{\cdot}015$, $x_0 = y_0 = -3$, and $\eta = 2^{11} = 2048$. The only firm requirement here was that η be a power of 2, which was required by the Fast Fourier Transform (FFT) routines that were used. The FFT were performed on the grid

$$s_j = j\Delta s, \tag{A 6}$$

$$\Delta s = 1/(\eta \Delta x), \tag{A 7}$$

where $j = 1, 2, \ldots \eta$.

The θ-integrations in (28) were performed via Gauss–Chebyshev quadrature [27]. The base points used were the roots of the 60th Chebyshev polynomial.

The final numerical detail to be discussed is that of convergence. Convergence was tested for by examining the parameter

$$\Delta S(r_i; j, m) = r_i \, | S_{\text{in}}(r_i; j, m) - S_{\text{out}}(r_i; j, m) | , \tag{A 8}$$

for each r_i, j, and m value set. It was required that $\Delta S(r_i; j, m)$ be less than or equal to 0·001 in all cases before convergence was said to have been reached.

Following a suggestion originally made by Broyles [30], the pth and $p + 1$st iterates were mixed to produce $S_{out}(r_i; j, m)$ by the use of a blend parameter, σ:

$$S_{out}(r_i; j, m) = S_p(r_i; j, m) + \sigma[S_{p+1}(r_i; j, m) - S_p(r_i; j, m)], \quad \text{(A 9)}$$

where $0 < \sigma \leqslant 1$. This $S_{out}(r_i; j, m)$ would then be used as the input for the $p + 2$nd iteration. It was found that the blend parameter needed to be small at high densities in order to achieve convergence. In other words, at high density the steps between iterates needed to be small in order that the iterative process be stable. Periodically, an extrapolated $S(r_i; j, m)$ was introduced in an effort to speed up convergence. $S(r; 0, 0)$ was typically the last coefficient to reach convergence.

References

[1] PRIESTLEY, E., WOJTOWICZ, P., and SHENG, P., 1974, *Introduction to Liquid Crystals* (Plenum).
[2] GELBART, W. M., 1972, *J. phys. Chem.* **86,** 4298.
[3] MAIER, W., and SAUPE, A., 1959, *Z. Naturf.* (*a*), **14,** 882; 1960, *Ibid.*, **15,** 287.
[4] ONSAGER, L., 1949, *Ann. N.Y. Acad. Sci.*, **51,** 627.
[5] STRALEY, J. P., 1971, *Phys Rev.* A, **4,** 675.
[6] TOBOCHNIK, J., and CHESTER, G. V., 1983, *Phys. Rev.* A, **27,** 1221.
[7] DENHAM, J. Y., LUCKHURST, G. R., ZANNONI, C., and LEWIS, J. W., 1960, *Molec. Crystals liq. Crystals*, **60,** 185.
[8] FRENKEL, D., and EPPENGA, R., 1985, *Phys. Rev.* A, **31,** 1776.
[9] FISHER, M. E., 1972, *Essays in Physics*, edited by G. K. T. Conn and G. N. Fowler (Academic Press).
[10] GRAY, C., and GUBBINS, K., 1984, *Theory of Molecular Fluids*, Vol. 1 (Oxford University Press).
[11] FRIES, P. H., and PATEY, G. N., 1985, *J. chem Phys.*, **82,** 429.
[12] LEE, L. Y., FRIES, P. H., and PATEY, G. N., 1985, *Molec Phys.*, **55,** 751.
[13] PERKYNS, J. S., FRIES, P. H., and PATEY, G. N., 1986, *Molec. Phys.*, **57,** 529.
[14] PERERA, A., KUSALIK, P. G., and PATEY, G. N., 1987, *Molec. Phys.*, **60,** 77.
[15] CHAKRAVARTY, S., and WOO, C.-W., 1975, *Phys. Rev.* A, **11,** 713; 1975, *Ibid.*, **12,** 245.
[16] LADO, F., 1982, *Molec. Phys.*, **47,** 283.
[17] LADO, F., 1982, *Molec. Phys.*, **47,** 299.
[18] LADO, F., 1982, *Molec. Phys.*, **47,** 313.
[19] VIEILLARD-BARON, J., 1972, *J. chem. Phys.*, **56,** 4729.
[20] BOUBLIK, T., 1975, *Molec. Phys.*, **29,** 429.
[21] STEELE, W. A., 1963, *J. chem. Phys.*, **39,** 3197.
[22] CAILLOL, J. M., LEVESQUE, D., and WEIS, J. J., 1981, *Molec. Phys.*, **44,** 733.
[23] ABRAMOWITZ, M., and STEGUN, I. A., 1972, *Handbook of Mathematical Functions* (Dover).
[24] CHEN, Y.-D., and STEELE, W. A., 1971, *J. chem. Phys.*, **54,** 703.
[25] CHEN, Y.-D., and STEELE, W. A., 1970, *J. chem Phys.*, **52,** 5284.
[26] WARD, D. A., 1986, Dissertation, North Carolina State University.
[27] PRESS, W. H., FLANNERY, B. P., TEUKOLSKY, S. A., and VETTERLING, W. T., 1986, *Numerical Recipes* (Cambridge University Press).
[28] LADO, F., 1968, *J. chem. Phys.*, **49,** 3092.
[29] TALMAN, J. D., 1978, *J. comput. Phys.*, **29,** 35.
[30] BROYLES, A. A., 1964, *J. chem. Phys.*, **40,** 939.